

Synthesis and Characterization of Trimanganese Tetraoxide Nanoparticles By Simple Chemical Route

¹ Annalakshmi N ²Anandhi Sarangapani

Department of physics

Faculty of Arts & Science

Bharath Institute of Higher Education and Research

Chennai India -600 073

[¹ lachuthuya@gmail.com](mailto:lachuthuya@gmail.com) [²Ananthi.Physics@bharathuniv.ac.in](mailto:Ananthi.Physics@bharathuniv.ac.in)

Address for Correspondence

¹ Annalakshmi N ²Anandhi Sarangapani

Department of physics

Faculty of Arts & Science

Bharath Institute of Higher Education and Research

Chennai India -600 073

[¹ lachuthuya@gmail.com](mailto:lachuthuya@gmail.com) [²Ananthi.Physics@bharathuniv.ac.in](mailto:Ananthi.Physics@bharathuniv.ac.in)

Abstract

Trimanganese tetraoxide (Mn_3O_4) nanoparticles have been prepared through simple chemical route. However, homogeneous nanoparticles of Mn_3O_4 are obtained. The crystallite size ranges from 20 and 30nm. In this material once subjected to a controlled annealing in water medium at $80^\circ C$ for concerning an hour yielded stage pure nanocrystalline particles of manganese tetraoxide and a pure tetragonal formation as revealed by a pattern of X-ray diffraction (XRD).

The HR- E M investigation ,reveals that the spherical morphological structure of Trimanganese tetraoxide and Energy Dispersive spectroscopy is used to identify that the composition of elements were present. The vibrational studies from FTIR measurements confirmed the presence of Mn-O bonding.

Keywords: Manganese chloride, XRD, HR-SEM, FT-IR, Nanocrystalline

Introduction

Materials at the nanoscale have recently taken up a lot of attention among researchers due to the single physical and chemical characteristics compared to the bulk counterparts. A nanomaterial is defined as any item with at least one dimension on the nanoscale. Nanomaterials are categorized according to their dimensions. Metal oxides have piqued material scientists' interest owing to the optical, electrical, thermal, magnetic, mechanical, and catalytic properties, which make them technologically important. Many important applications for metal oxides such as iron, nickel, cobalt, manganese, copper, and zinc have been studied, including magnetic storage media, solar energy transformation, electronics, semiconductors, and catalysis.

Manganese Oxide(MnO)Nanoparticles

Manganese exists in a number of states of oxidation as well as the formation of chemical structure. Because of their strong reducing potential, manganese oxides are also aggressive oxidants. Only a combination of different manganese oxides (MnO_2 , Mn_2O_3 , and Mn_3O_4) is generally produced due to the diversity of oxidation states and the rapid phase transitions of MnO_x during production. [Wells, 1987].

A manganese oxide is one of the majority common natural resources on the world and it may be found in a wide range of natural sediments, soils and ores. It has also been found in desert rock varnish and marine manganese oxides [Achurra 2009]. There are many naturally occurring crystalline manganese oxides with close MnO_2 stoichiometry, as well as several amorphous manganese oxides [Achurra 2009, Luo 2008, Nitta 1984, and Cao 2010.]. Furthermore, crystalline material architectures are mostly composed of edge-shared MnO_6 octahedral units that are organized to resemble tunnelled or layered structures. MnO contributes towards the far above the ground porosity with surface area of the material's structure.

Application of Manganese Oxide Nanoparticle:

Among them, Manganese Oxide (MnO) has a wide range of potential uses in both industrial and commercial settings. Manganese (Mn) oxide is the most powerful natural oxidant agent and may be found in a variety of natural habitats and oxidation states such as $Mn(II)$, $Mn(III)$, and $Mn(IV)$ and is connected to their oxidation state, crystalline phase, and surface area. [2019] Vicentede Oliveira Sousa Neto. Because of its excellent corrosion resistance, Mn_3O_4 has uses

in catalysis, hazardous waste cleanup, as additives in refractory, paint, and superconductor goods, and in steel manufacture [Kumari et al., 2009]. Manganeseoxide nanoparticles have piqued the interest of researchers corresponding to the potential uses in electrical, optical, and mechanical devices based on changing oxidation states. Metal oxide nanopowder is synthesised using several techniques, although published procedures have little control over particle functioning [Lind., 1988].As a result, it is critical to change the cost-effective method in a chemcialsubstance and environmentally forthcoming way.

Materials and Methods

Chemicals

Manganese Chloride hexa chloride [$\text{Mn}(\text{Cl}_2)_2 \cdot 6\text{H}_2\text{O}$], the precursor for Manganese, Sodium hydroxide (NaOH), the oxide source, Ethanol, Deionized Water were purchased from Merck. Because the chemicals were of analytical reagent grade with 99 percent purity, they were utilised exactly as received.Simple chemical route was used to synthesize manganese oxide nanoparticles. X-ray powder diffraction method FTIR, HRSEM and EDAX were used to characterize structural and morphologicalwith chemical compositions studies respectively.

Preparation of Manganese Oxide NPs .

For the production of nanosized MnO precursors, 1M of Manganese chloride (MnCl_2) in 100ml of deionized water and 0.75 M in 100ml of NaOH were combined and rapidly stirred at 30oC. After 8 hours of stirring, a brown precipitate of MnO precursor was produced. To eliminate contaminants, the obtained precursor was washed with deionized water and ethanol alternately. To obtain the nano-sized powder of precursor MnO, the washed product was kept at 80°C in a hot air oven. The precursor was annealed at 500°C for 4 hours to get the pure phase of MnO. To make nano-sized MnO particles.

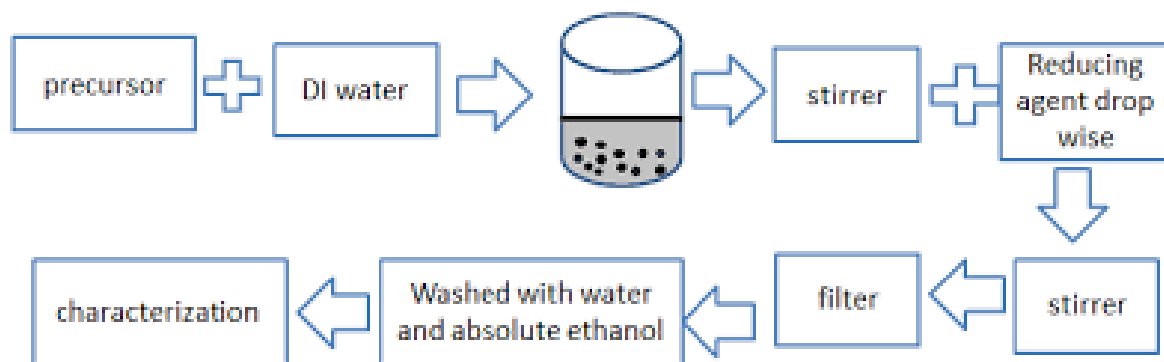
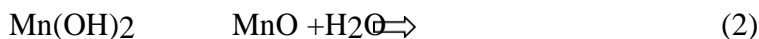
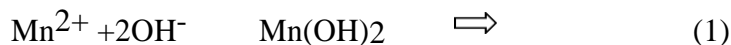


Fig1. Flow chart for preparation of manganese nano particles



The above Manganese ions are initially concentrated in alkaline solution. After that, manganese hydroxide is produced, which decomposes into MnO. Later, ambient oxygen oxidises MnO to become Mn₃O₄. The nanomaterials were then examined using X-Ray patterns (XRD) using Cu-K1 radiation in the 2θ range of 20° – 90°, Fourier Transform infrared spectroscopy in the area 4000 – 400cm⁻¹ with High Resolution scanning electron microscopy (HR-SEM).

X-Ray Diffraction (XRD)

Fig.3.1 show the XRD pattern is utilised to identify the phase and purity of the produced Mn₃O₄ nanoparticles

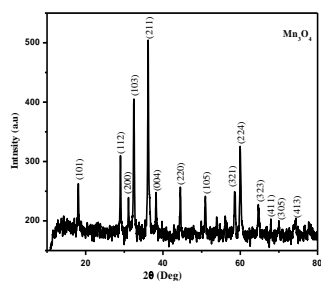


Fig XRD particle diffraction pattern

The diffraction peaks are extremely broad hump and have a very low intensity, implying that the size of the produced Mn₃O₄ nanoparticles is quite tiny [Y.Li, H.Tan 2011]. The presence of nano-size particles is indicated by significantly widened lines in the XRD patterns. We utilised the (101), (112), (103) (211), and (224) reflections, as shown in XRD patterns, to

calculate the average particle size using Debye–eqn.(2) Scherrer's [Park et al., 2004]. The Mn₃O₄ lattice constants found by refinement of the nanomaterial XRD statistics are a equal to b is 5.7630 and c is 9.4560, which are steady with conventional ethics for bulk Mn₃O₄ [Chowdhury 2009]. They also agree with the published values of Mn₃O₄ [G.An., P.YU, 2008] for particles, indicating that the sample was produced in a single phase. Crystallite size of Mn₃O₄

The crystallite size of Mn₃O₄ is taken into account by appropriate the synchrotron

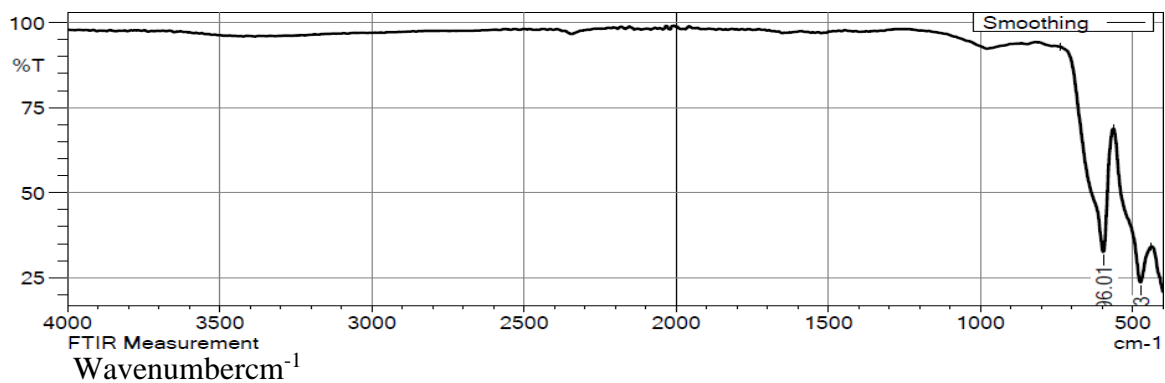
$$D_p = \frac{0.94\lambda}{\beta_{1/2} \cos \theta}$$

XRay pattern data with the equation of Debye-Scherrer

Where, θ =Braggangle, $\lambda=1.5406\text{nm}$ =wavelengthofX-ray, $\beta_{1/2}$ =FullWidth Half- maxima (FWHM), D_p = crystallite size ofparticle. Where whole width at is half highest of the crest in the XRD pattern, is the diffraction angle, and is the X-ray wavelength. The structural characteristics for the Mn₃O₄ samples, such as lattice constant, disorder density, and micro strain, were computed and are reported in Table 3.1. In terms of micro strain, smaller particles have a greater strain value, whereas bigger particles have a lower strain value.

Functional group Using FTIR

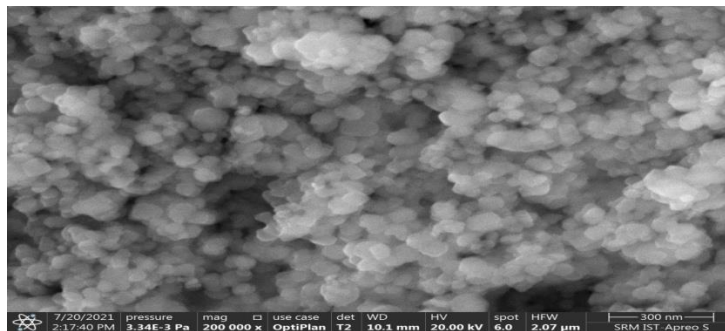
Fig.3.5 depicts the spectroscopy of FT-IR of produced Mn₃O₄ nanoparticles..The stretching of Mn-O modes is Tetrahedral and Octahedral units may be ascribed to the distinctive vibrational mode of two wide absorption peaks situated at 473.51cm⁻¹ and 596.12cm⁻¹. The vibrational mode at 473.51 cm⁻¹ is caused by bending vibration, whereas the vibrational mode at 596.01 cm⁻¹ is caused by stretching vibrations is bond is Mn–O in MnO₆ octahedral. The presence of hydroxyl stretching vibrations causes the high absorption peak at 3410 cm⁻¹. The peak is weak absorption found around 1629 cm⁻¹ refers to moisture adsorption on the plane of the sample, whereas a tiny peak at 1372 m⁻¹ belongs to OH bending vibrations coupled with Mn atoms .



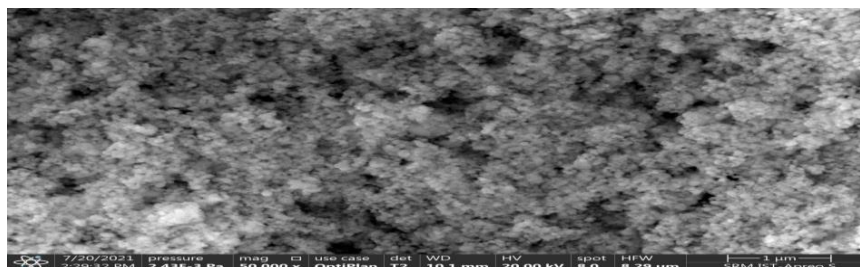
.FTIR Spectrum of Mn_3O_4 nanoparticles

HR-SEM:

Using a High Resolution Scanning Electron Microscope (HRSEM), the morphology, particle size, and crystallinity of Mn_3O_4 nanoparticles were studied (Fig. 3.6). The particles' sizes have a spherical shape, as seen in the picture below.



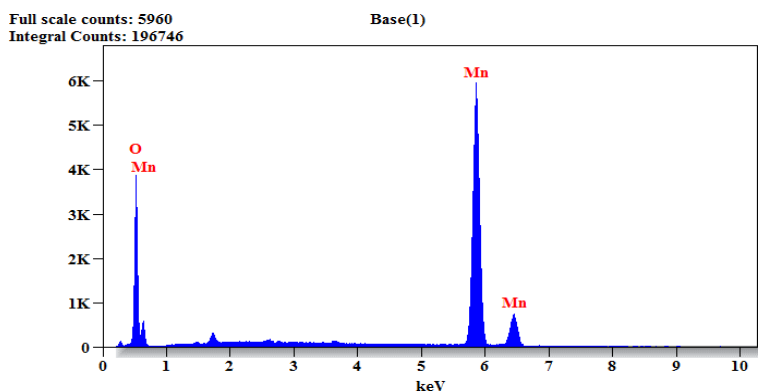
(a)



(b)

Fig. 3)a&B -.HR-SEM Images of Mn₃O₄**Elemental composition of brown Mn₃O₄**

It can also detect the presence of manganese and oxygen atoms in nanoparticles. Because of the concentration of chemical substance is obtained from the Energy Dispersive spectrum, it can be determined so as to the produced sample's concentration is Mn₃O₄ and no foreign elements were present.

Fig.3.7EDX spectrum of Mn₃O₄**CONCLUSION**

The present study demonstrates the effect of the structural, morphological, and functional properties of Mn₃O₄ nanostructures prepared through a simple chemical precipitation route. Additionally, the products annealed at 500°C were analyzed for their structural, morphological, and functional group analysis. The XRD patterns revealed that the particles exhibit a pure cubic structure. The estimated sizes of the nanoparticles were in the range of 20-30 nm. The FTIR spectra confirmed the formation of the MnO nanostructures. HR-SEM analysis shows the formation of spherical shape morphology with sizes ranging between 20 and 30 nm. In this viewpoint, applications of the synthesized nano materials containing photocatalysis (e.g. reduction of CO₂, degradation of CH₃CHO, dye degradation, etc), dye process in sensitized solar cells, lithium battery, supercapacitor in nanofluids with highly thermal conductivity, of heavy metal ions removal and MRI.

REFERENCES

1. H. Willard, L. Merrit, J. Dean, and F. Settle, "Instrumental methods of analysis" CBS publishers and distributors India, First Indian edition, 1986.
2. W. Wesley, M. Wendlandt, Thermal Analysis (Wiley, New York, 1964).
3. .Bhushan, B "Handbook of Nanotechnology", publisher Springer, 1-5 (2010).
4. Wang, J., M. Lin, Y. Yan, Z. Wang, P.C. Ho, K.P. Loh, "CdSe/AsS Core-Shell Quantum Dots: Preparation and Two-Photon Fluorescence," J. Am. Chem. Soc., 131,11300-11301, (2009).
5. Kim, Y.T., J.H. Han, B.H. Hong, Y.U. Kwon, "Electrochemical synthesis of Cd-Se quantum-dot arrays on Graphene basal plane using mesoporous silica thin-film templates," Adv. Mater., 22, 515-518, (2010).
6. Wang, Y., Q.Z. Qin, "A Nanocrystalline NiO Thin-Film Electrode Prepared by Pulsed Laser Ablation for Li-Ion Batteries," J. Electrochem. Soc. 149(7), A873-A87, (2002).
7. Compagnini, G., A.A. Scalisi, O. Puglisi, "Production of gold nanoparticles by laser ablation in liquid alkanes," J. Appl. Phys. 94, 7874-7877, (2003).
8. Dahl, J.A., B.L.S. Maddux, J.E. Hutchison, "Toward Greener Nano synthesis", Chem. Rev. 107, 2228-2269, (2007).
9. Shah, M.A., T. Ahmad, "Principles of Nanoscience and Nanotechnology", Narosa Publishing House, 32-65, (2010).
10. Jadhav, A.P., C.W. Kim, H.G. Cha, A.U. Pawar, N.A. Jadhav, U. Pal, Y.S. Kang, "Effect of Different Surfactants on the Size Control and Optical Properties of Y₂O₃:Eu³⁺ Nanoparticles Prepared by Coprecipitation Method," J. Phys. Chem. C.113, 13600–13604 (2009).
11. Kim, Y.T., J.H. Han, B.H. Hong, Y.U. Kwon, "Electrochemical synthesis of Cd-Se quantum-dot arrays on Graphene basal plane using mesoporous silica thin-film templates," Adv. Mater., 22, 515-518, (2010).
12. Hankache, J. & Wenger, O.S. "Organic Mixed Valence", Chem. Rev. 111, 5138-5178 (2011).

13. Young, C.G., (1989) “Mixed-valence compounds of the early transition-metals”*Coordination Chemistry Reviews.*, 96, 89-251.
- 14 Varma, C.M “Mixed-valence compounds”,*Reviews of Modern Physics.*, 48, 219-238., (1976).
- 15.L.E. Foster, “Nanotechnology”, *Personal Education, New Delhi*, (2006) 143-145. 42
16. L. Ren, Y.P. Zeng, D. Jiang, *Solid State Sci.* 12, 138–143., (2010).
17. G.Q. Zhang, N. Chang, D.Q. Han, A.Q. Zhou, X.H. Xu, *Mater. Let*
- 18.R. Ramachandran, *J. Mater. Sci.: Mater. Electron.* 13 (2003) 257. 23. M. Drofenik, A. Žnidaršič, M. Kristl, A. Košak, D. Makovec, *J. Mater.Sci.* 38 (2003) 3063.
19. S. Fritsch, J. Sarrias, A. Rousset, G.U. Kulkarni, *Mater. Res. Bull.* 33(1998) 1185.
20. O.Y. Gorbenko, I.E. Graboy, V.A. Amelichev, A.A. Bosak, A.R. Kaul, B.Güttler, V.L. Svetchnikov, H.W. Zandbergen, *Solid State Commun.*124 (2002) 15.
21. V. Berbenni, V. Marini, *Mater. Res. Bull.* 38 (2003) 1859.
22. J.M. Boyero, E.L. Fernández, J.M. Gallardo-Amores, R.C. Ruano, V.E. Sánchez, E.B. Pérez, *Int. J. Inorg. Mater.* 3 (2001) 889.
23. F.A. Al Sagheer, M.A. Hasan, L. Pasupulety, M.I. Kaki, *J. Mater. Sc Lett.* 18 (1999) 209.
24. E.R. Stobbe, B.A. de Boer, J.W. Geus, *Catal. Today* 47 (1999) 161.